

Design Study of the Bending Sections between Harmonic Cascade FEL Stages *

W. Wan, J. Corlett, W. Fawley, A. Zholents, LBNL, Berkeley, CA 94720, USA

Abstract

The present design of LUX (linac based ultra-fast X-ray facility) includes a harmonic cascade FEL chain to generate coherent EUV and soft X-ray radiation. Four cascade stages, each consisting of two undulators acting as a modulator and a radiator, respectively, are envisioned to produce photons of approximate wavelengths 48 nm, 12 nm, 4 nm and 1 nm. Bending sections may be placed between the modulator and the radiator of each stage to adjust and maintain bunching of the electrons, to separate, in space, photons of different wavelengths and to optimize the use of real estate. In this note, the conceptual design of such a bending section, which may be used at all four stages, is presented. Preliminary tracking results show that it is possible to maintain bunch structure of nm length scale in the presence of errors, provided that there is adequate orbit correction and there are 2 families of trim quads and trim skew quads, respectively, in each bending section.

INTRODUCTION

The present design of LUX ([1, 2, 3, 4]) includes a harmonic cascade FEL chain to generate coherent EUV and soft X-ray radiation. Four cascade stages, each consisting of two undulators acting as a modulator and a radiator, respectively, are envisioned to produce photons of wavelengths 48 nm, 12 nm, 4 nm and 1 nm ([3, 4]). Four bending sections are placed between the modulator and the radiator of each stage to adjust and maintain bunching of the electrons, to separate, in space, photons of different wavelengths and to optimize the use of real estate. In this note, the conceptual design of such a bending section, which can be used at all four stages, is presented. Preliminary tracking results show that it is possible to maintain bunch structure of the length 1 nm with the presence of errors, provided that there is adequate orbit correction and there are 2 families of trim quads and trim skew quads, respectively, in the bending section.

LAYOUT

First of all, the length scale of 1 nm is at least an order of magnitude shorter than any study appeared before ([6, 7]). There is no doubt that all second order aberrations in time-of-flight have to be corrected. It remains to be seen whether higher order aberrations are small enough. The most efficient way of achieving this goal, to the mind of the author at least, is to take full advantage of the four cell achromat first

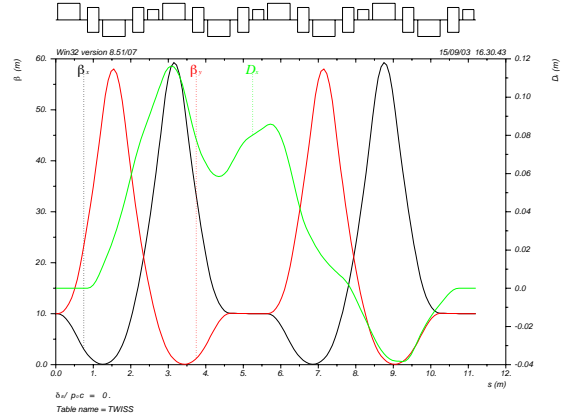


Figure 1: Plots of the lattice functions using MAD [8]

systematically studied and applied in realistic design by K. Brown ([5]). The basic result is that a beamline is an achromat if it consists of 4 identical FODO cells with 90 degree phase advance in both planes. To the first order, time-of-flight depends on momentum only ($R_{56} \neq 0$). If 2 families of sextupoles are added to correct chromaticity, to the second order, time-of-flight depends on momentum only ($T_{566} \neq 0$). To maintain bunch structure at the 1 nm level, both R_{56} and T_{566} have to be under control, which means that one extra knob each on the first and second order optics. It is certain that at 2.5 GeV, the knob to adjust T_{566} has to be a sextupole. Yet there are at least two options to cancel and adjust R_{56} . To cancel R_{56} , or to make R_{56} very small, which is the case here, either negative dispersion has to be created or reverse bends have to be used. Generally speaking, using reverse bends requires weaker quadrupoles. It was found that third order aberrations are too large if negative dispersion is used to cancel R_{56} . To adjust R_{56} , one option is to use an additional family of quads, which was not adopted due to the concern of the cost and the length of the beamline. The scheme used here is the redistribution of bending (keeping the total bending fixed). As a result, the bending section consists of 4 identical cells. Each cell contains 2 dipole, 2 quadrupole and 3 sextupole magnets. The total bending angle of the beamline is 5 degrees. It turns out that, at sub-micron level, adjusting R_{56} does not affect focusing, making it an independent knob. To shorten the length further, two families of sextupoles are placed inside the quads. The spacing between magnets is 10 cm, except that, after each quad, an extra 10 cm is reserved for BPM and correct/skew quad coils. The characteristics of the electron beam is summarized in Table 1, the key parameters of all main magnets are listed in Table 2 and the lattice functions are shown in Fig. 1.

* Work supported by the Director, Office of Energy Research, Office of Basic Energy Science, Material Sciences Division, U.S. Department of Energy, under Contract No. DE-AC03-76SF00098

Beam energy (GeV)	2.5
Bunch charge (nC)	1
Full bunch length (ps)	2
Beam energy modulation (keV)	± 2.5
Normalized emittance (m-rad)	$3e-6$

Table 1: List of beam parameters

Type	Length (cm)	Field at 1.5 cm (kG)
Bend (B1)	30	12.7375
Bend (B2)	30	-6.6243
Quad (QF)	60	-2.5513
Quad (QD)	60	2.5423
Sextupole (S1)	60	0.7297
Sextupole (S2)	60	1.5768
Sextupole (S3)	30	-3.6514

Table 2: List of magnets (trims not included), along with their lengths and strengths

PERFORMANCE

Preliminary tracking study has been done to evaluate the performance of the beamline. Since the bending section upstream the last stage is the most difficult to achieve, results from this bending section only are presented. The initial distribution of electrons is the output of a simulation that models the effect of a FEL modulating the beam at the wavelength of 4 nm. The energy of the beam is 2.5 GeV, the normalized transverse emittance (round beam) is $3 \pi \text{ mm mrad}$ (see also Table 1) and the peak to peak energy modulation is 5 MeV. The simulation is performed using the code COSY INFINITY [9]. First, the effect of the remaining aberrations beyond the second order is examined. The effect of the fringe field is also checked using the default model provided by the code ([9]). The result is shown in Fig. 2 and 3. It is obvious from Fig. 3 that, regardless the model of the fringe field, the remaining aberrations are small enough to maintain the bunch structure at 1 nm level.

The effect of errors is simulated through computer generated random Gaussian distribution. Up to now, only static errors are included, which are the setting errors of the dipoles, quadrupoles and sextupoles, the sextupole component in dipoles and quadrupoles, tilt and misalignment of quadrupoles and sextupoles. Unless stated otherwise, the RMS values of the errors are shown in Table 3. The cutoff is 2.5σ . In order to ensure success in operation, dipole, quadrupole (normal and skew) and sextupole correctors are included in the design. Trim coils are envisioned in each quad and 2 families of sextupoles that are inside the quads. A slot of 10 cm downstream of each quad is reserved for a BPM and a set of dipole corrector/skew quad coils. The currents of the main dipoles are used to restore R_{56} to the optimal value. Specifically, there are 8 horizontal dipole correctors and 8 vertical correctors, all of which are individually powered. The trim quads, skew

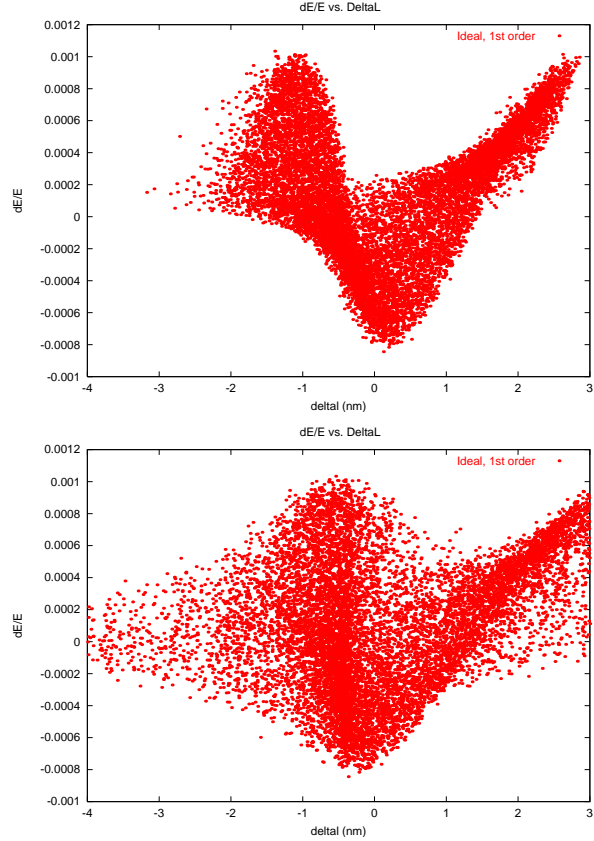


Figure 2: Distribution of particles in the longitudinal phase space (no errors); upper left: initial distribution; upper right: distribution at the end of the beamline using the linear matrix; lower left: distribution at the end of the beamline using the 5th order map with the tails cut off; lower: same as the previous plot except that the tails are included.

quads and trim sextupole are grouped into 2 families, respectively. In one family, the elements are powered symmetrically about the midpoint of the beamline and, in the other family, they are powered anti-symmetrically. The 2 currents of the main dipoles are group into 1 family, keeping the difference fixed, hence the total bending angle unchanged.

It is shown in Fig. 5 that, with errors listed in Table 3, bunch compression can be restored when trim quads, skew quads and trim sextupoles are turned on and the dipole correctors are off. Fig. 4 shows that, without orbit correction, both trim and skew quads have to be on to maintain the short bunches.

DISCUSSION

A design of the bending sections between the stages of harmonic cascade FEL is presented. In order to maintain the bunch structure at 1 nm, all second order aberrations are corrected. To reduce remaining aberrations, reversed dipoles are used. With 2 families of trim quads, skew quads and trim sextupoles, respectively, the effect of static errors

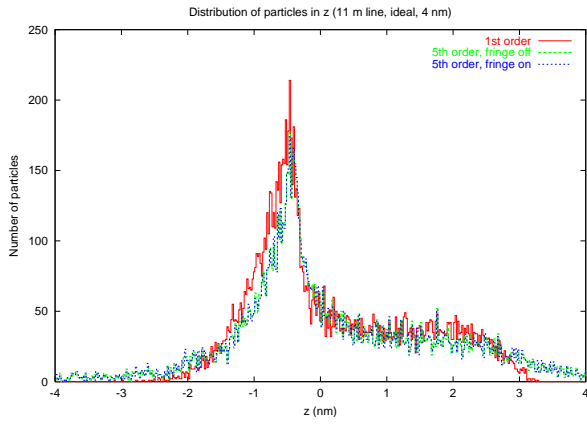


Figure 3: Histograms showing the longitudinal distribution after the ideal beamline. The full-width-half-maximum (FWHM) is 0.50 nm, 0.50 nm and 0.49 nm, for the cases of first order map, fifth order map without fringe field and fifth order map with fringe field, respectively.

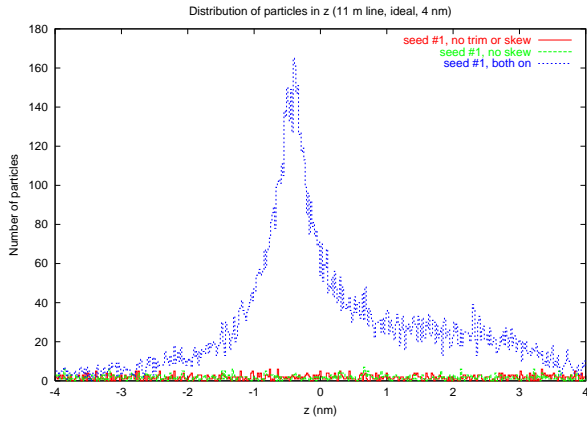


Figure 4: Histograms showing the longitudinal distribution after the beamline when errors are included. red: both trim and skew quads are off; green: trim quad are on but skew quads are off; blue: both trim and skew quads are on. Note that the difference of the time of flight of the reference particle among different seeds, which is irrelevant, are subtracted. This is true for other plots as well.

can be effectively corrected. Implementation remains the outstanding issue. A practical scheme is yet to be developed to tune up the beamline and maintain stable operating conditions over time.

ACKNOWLEDGMENT

The author would like to thank R. P. Wells, A. Wolski and for numerous stimulating discussions.

REFERENCES

[1] J. Corlett et al., “Feasibility Study for A Recirculating Linac-based Facility for Femtosecond Dynamics”, LBNL formal report LBNL-51766, December 2002.

Type	Amplitude
setting errors (all magnets)	$\sigma(\frac{\Delta B}{B}) = 1e-3$
sextupole (dipoles)	$\sigma(\frac{b_3}{b_1}) = 2.5e-5$ (1.5 cm)
sextupole (quads)	$\sigma(\frac{b_3}{b_2}) = 1.5e-4$ (1.5 cm)
tilt	$\sigma(\Delta\phi) = 0.2$ mrad
misalignment (transverse)	$\sigma(\Delta x), \sigma(\Delta y) = 30$ μ m
misalignment (longitudal)	$\sigma(\Delta l) = 1$ mm

Table 3: List of errors included in the simulation and their amplitudes.

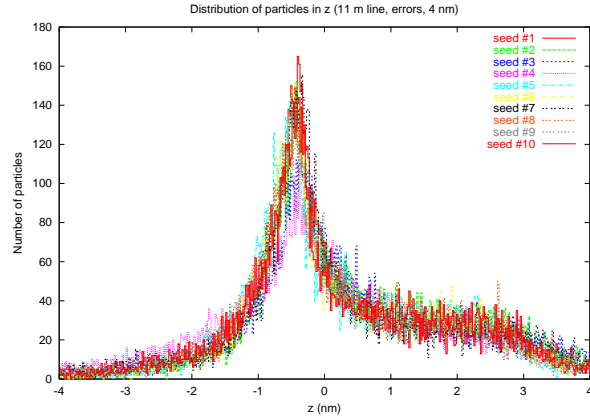


Figure 5: Histogram showing distributions of 10 sets of errors. All correctors except the dipole correctors are on.

[2] J. Corlett et al. “A Recirculating Linac-Based Facility for Ultrafast X-Ray Science”, in Proc. 2003 Particle Accelerator Conference, in press.

[3] W. M. Fawley, W. A. Barletta, J. N. Corlett and A. Zholents, “Simulation Studies of A XUV/Soft X-Ray Harmonic-Cascade FEL for the Proposed LBNL Recirculating Linac”, in Proc. 2003 Particle Accelerator Conference, in press.

[4] A. A. Zholents, J. N. Corlett, W. Fawley and J. Wurtele, *Beam Transport Lattice in a Cascaded Harmonic FEL* CBP Tech Note-281, February 2003.

[5] K. L. Brown, *A Second-Order Magnetic Optical Achromat*, IEEE Transactions on Nuclear Science, NS-26, No. 3, p3490 (1979).

[6] S. Chattopadhyay, C. Kim, D. Massoletti, W. Wan, A. Zholents and M. Zolotarev, *Proposal for Experimental Test of Optical Stochastic Cooling Scheme*, LBNL formal report, LBNL-39788, January 1997.

[7] A. Zholents, M. Zolotarev and W. Wan, *Generation of Attosecond Electron Bunches*, in Proc. 2001 Particle Accelerator Conference, 723 (Chicago, 2001).

[8] H. Grote and C. F. Iselin, *The MAD Program (Methodical Accelerator Design) Version 8.16, User's Reference Manual*, CERN/SL/90-13 (AP) (Rev. 4) 1995.

[9] M. Berz and K. Makino, *COSY INFINITY Version 8.1 Users Guide and Reference Manual*, MSUHEP-20704, Dept. Physics and Astronomy, Michigan State University, 2002.